# Minimal impact of model biases on northern hemisphere ENSO teleconnections.

Nicholas L. Tyrrell[1], Alexey Yu. Karpechko[1]

[1]Finnish Meteorological Institute, Helsinki, 00500, Finland

5 *Correspondence to*: Nicholas L. Tyrrell (nicholas.tyrrell@fmi.fi)

**Abstract.** Correctly capturing the teleconnection between the El Niño–Southern Oscillation (ENSO) and Europe is of importance for seasonal prediction. Here we investigate how systematic model biases may affect this teleconnection. A two–step bias–correction process is applied to an atmospheric general circulation model to reduce errors in the climatology. The bias–corrections are applied to the troposphere and stratosphere separately and together to produce a range of climates.

10 ENSO type sensitivity experiments are then performed to reveal the impact of differing climatologies on ENSO–Europe teleconnections.

The bias–corrections do not affect the response of the tropical atmosphere nor the Aleutian Low to the strong ENSO anomalies imposed in our experiments. However, the anomalous upward wave flux and the response of the northern hemisphere polar vortex differ between the climatologies. We attribute this to a reduced sensitivity of the upward wave

15 fluxes to the Aleutian Low response in the bias-correction experiments, where the reduced biases results in a deepened Aleutian Low in the base state. Despite the differing responses of the polar vortex, the NAO response is similar between the climatologies, implying that for strong ENSO events a stratospheric pathway may not be necessary for the ENSO–North Atlantic teleconnection.

# 1 Introduction

20   The El Niño–Southern Oscillation (ENSO) has been shown to influence European climate via tropospheric and stratospheric teleconnections. Although ENSO is a key driver of global variability on seasonal to annual timescales it's effect on Europe is less robust (Brönninman 2007), and exhibits decadal variability (Rodríguez–Fonseca et al., 2016). The large seasonal variability in the mid–latitude Northern hemisphere, and relatively low number of observed ENSO events create some difficulty in measuring the effect in observational data. The ENSO–Europe teleconnection begins with anomalous

25   convection in the tropical Pacific, and during El Niño events this leads to increased divergence in the upper troposphere, creating a Rossby wave source (Hoskins and Karoly, 1981). The anomalous Rossby waves propagate to the Northern Pacific where they strengthen the wintertime Aleutian Low. There are multiple possible connections between the North Pacific anomalies and the North Atlantic (Jiménez–Esteve and Domeisen, 2018), with a tendency for a negative North Atlantic Oscillation during El Niño event. For the stratospheric connection, as reviewed by Domeisen et al., (2019), the deepened

30   Aleutian low can lead to upward propagating waves, particularly of wavenumber 1, which travel into the stratosphere and weaken the wintertime stratospheric polar vortex. For strong vortex weakening events, such as sudden stratospheric warmings, anomalies can propagate down to the troposphere and project onto the Northern Annular Mode, and the North Atlantic Oscillation (NAO) (Butler et al., 2014). The result is also a tendency for a negative NAO during El Niño events. The opposite is approximately true for La Niña events, but the anomalous response is weaker (e.g. Jiménez–Esteve and

35   Domeisen, 2019). Mezzini et al. (2020) suggest the NAO-like patterns that result from ENSO variability are distinct from the NAO, and result from a Rossby wave train from the tropics to the North Atlantic which does not affect NAO variability.

Both the tropospheric and stratospheric teleconnection pathway can be simulated with climate models of sufficient resolution (Cagnazzo and Manzini, 2009, Bell et al. 2009). Models also allow for large numbers of ENSO events to be simulated, which has revealed non–linearities in teleconnections (Frauen, et al. 2014, Jiménez–Esteve and Domeisen, 2019, Garfinkel et

40   al 2019). However, for confidence in modelling results, we need an understanding of the deficiencies of models. A fully coupled model needs to correctly represent both the complex dynamics of the ENSO ocean–atmosphere interactions to generate the convective anomalies that drive the teleconnections, and the mean climatology so the anomalies interact with the base state correctly. For example, the convective response of tropical Pacific is dependent on the mean state of the Walker circulation (Bayr et al. 2018). The location and strength of the convective response is then important in controlling

45   the location of the extratropical pressure response (Bayr et al., 2019), and can lead to non–linearities. In addition to the patterns of climatological SSTs, the state of the tropical (e.g. Quasi-Biennial Oscillation (QBO) phase) and extratropical atmosphere can influence the response of the NAO and polar vortex (Garfinkel et al., 2007).

The technique of flux correcting SSTs has been used to study the effect of model biases on ENSO dynamics (Spencer et al., 2007, Magnello and Huang, 2009, Dommenget et al., 2014) or seasonal forecasting (Magnusson et al., 2013a, Magnusson et

50   al., 2013b). Empirical corrections are added to the coupling between the ocean and atmosphere to push the model towards

the observed climatology. It is possible to use a similar technique on the prognostic atmospheric variables of a model. This bias–correction technique was used by Kharin and Scinocca (2012), and artificially decreased biases were associated with an increase in predictive skill on seasonal timescales. Simpson et al., (2013a, 2013b) used the technique to study the impact of jet latitude bias on the Southern Annular Mode (SAM), although they did not see improvements in the persistence of the SAM when they reduced biases in the jet. When Chang et al. (2019) used a similar bias–correction technique they found an improvement in the North Pacific jet and North American rainfall climatology, and a modest improvement in seasonal forecast skill. Tyrrell et al., (2020) investigated how climatological biases effect the relationship between the Eurasian snow extent and the wintertime polar vortex. The strength of the vortex was found to have only a small effect on its response to a tropospheric forcing, however the downward propagation of stratospheric anomalies was sensitive to the tropospheric circulation.

In this study we have used a similar bias correction technique to probe the impact of climatological biases on the communication of ENSO anomalies from the tropical Pacific to the North Atlantic and European sector. The technical details of the model and experiments are described in section 2, the results of the bias corrections and ENSO experiments are described in section 3, and a discussion and conclusions are presented in section 4.

## 2 Data and Methods

We use the ECHAM6 spectral atmospheric model (Stevens et al., 2013), run with a horizontal truncation of T63 and 95 vertical levels with a model top at 0.02 hPa. The bias correction technique follows Kharin and Scinocca, 2012, and is similar to that described in Tyrrell et al., 2020 (T20). It is a two–step process; first, the bias correction terms are calculated in a nudged training stage. The model's prognostic variables – divergence, vorticity, temperature, and log of surface pressure – are nudged towards ERA–Interim for 30 years and the nudging tendencies are recorded every 6 hours. Then the nudging tendencies are used to create a climatology of correction terms. This climatology is then smoothed in time with a Gaussian filter with a 25 day window, and it represents the inherent bias in the model's prognostic variables. Secondly, the climatology of correction terms is added to the free running model as an additional tendency term at each time step. An important difference between the nudged and bias corrected runs is that the bias correction terms are independent of the current model state, so the model can respond to perturbations, whereas during the nudged run the model is tightly constrained to the reanalysis. The technical details of the bias correction are outlined in T20, with two differences for the current experiments. For the training step the model was nudged to ERA–Interim data from 1979–2009, whereas in T20 only the years 1979–1989 were used. This did not impact the results, with the resulting bias correction terms being very similar. The second difference to T20 was that the only bias correction terms used for this study were the divergence and temperature, rather than the divergence, vorticity, temperature and log of surface pressure. During the training stage all the model's prognostic variables were nudge towards ERA Interim, but it was found that using only two of the temperature, divergence and vorticity of the bias correction terms gave the best results for reducing the biases in the winds and

temperature. Through testing different combinations we found that bias correcting only the divergence and temperature lead to the biggest decreases in the climatological biases of the control run.

85    The bias corrections were applied on model levels between approximately 850 hPa and 2.6 hPa, and three types of bias correction runs were performed; the troposphere and stratosphere were corrected in FullBC, the stratosphere only in StratBC, and the troposphere only in TropBC (see Table 1 for details). Then ENSO SST forcing experiments were conducted with each of these bias corrected climatologies. To generate the SST pattern we used a regression of the Niño3.4 timeseries and HadISST SSTs from 1979–2009. Only positive regression values between 30°S and 30°N and east of 150°E in the Pacific

90    Ocean were used for the pattern, and the regression values were multiplied by 1.5 to strengthen the response, which corresponds to an El Niño or La Niña forcing magnitude of 1.5K. Climatological SSTs, using HadISST data from 1979-2009, were used for the CTRL run. The ENSO pattern was added to (El Niño), or subtracted from (La Niña) the SST climatology in the tropical Pacific, with climatological SSTs used everywhere else. The ENSO pattern was kept constant in time, i.e., the anomaly did not vary seasonally. Each experiment was run for 100 years. It should be noted that using a

95    regression to generate ENSO patterns results in symmetric El Niño/La Niña magnitudes, whereas from observations El Niño anomalies tend to be larger than La Niña. This simplification, along with a constant ENSO forcing and climatological SSTs outside the Pacific Ocean basin, has the advantage of reducing the number of controlling parameters when analysing the results of the bias-corrections, which was the main aim of the research. However, the simplifications should be considered when comparing the results with observations, particularly in relation to the intra-seasonal and early winter ENSO-Atlantic

100    connection (e.g. King et al., 2018) that may be driven by SSTs and rainfall away from the Pacific (Ayarzagüena et al., 2018, Abid et al., 2021).

To calculate the root-mean-square error and biases between the model and reanalysis (Fig. 1) we use ERA Interim 1979–2009, since that data was used for our bias correction scheme. However, when analysing the response to El Niño and La Niña runs, the newer ERA5 data is used (Hersbach et al., 2020), since it is a longer time series. To divide the data the

105    NINO3.4 index was used for DJF (https://origin.cpc.ncep.noaa.gov/products/analysis_monitoring/ensostuff/ONI_v5.php). El Niño years defined as NINO3.4 above 0.9 K (8 years), La Niña years NINO3.4 below -0.9 K (8 years) and the years between -0.5 K and 0.5 K were defined as neutral years (13 years). The slightly stricter threshold of +/- 0.9 K was used to define the El Niño/La Niña years to include only stronger events.

## 3 Results

110    ### 3.1 Reduced model biases

The climatological biases of the model's wind and temperature vary with latitude and height. In Fig. 1 we show the root mean square error (RMSE) of the zonal mean zonal wind (UZ) for three regions; the tropics (20°S – 20°N), mid–latitudes (20°N – 50°N) and the polar region (50°N – 90°N; the polar region is extended to 50°N to capture the full extent of the stratospheric polar vortex). The RMSE is calculated relative to the 1980–2009 ERA Interim climatology. It should be noted

that the control run (green dashed line) performs very well in many regions, particularly the tropics, with UZ RMSE values below 2 m s$^{-1}$. The errors are small in the lower troposphere, and tend to increase with height. In Fig. 1 panels d–e we show the percentage change in the UZ RMSE, between the CTRL run and the three bias–corrected runs. These figures demonstrate the effectiveness of the different height–dependent bias correction experiments. For example in Fig. 1e, in the mid–latitudes the corrections in the TropBC experiment reduce the UZ RMSE by around 40% in the troposphere. Although the corrections stop at around 100 hPa their effect continues into the stratosphere, but weakens. As the tropospheric corrections weaken, the corrections in StratBC lead to around a 25% decrease in UZ RMSE in the upper stratosphere. In the mid-latitudes FullBC the UZ RMSE is reduced throughout the atmosphere with reductions of over 50% in the upper troposphere–lower stratosphere region. The same is somewhat true for the tropics and polar regions, although with some exceptions such as the tropical stratosphere, where errors are increased in the FullBC and TropBC, which may be related to the QBO. In the polar atmosphere, the improvements in the FullBC are mostly seen between 100-200 hPa and in the upper stratosphere. The TropBC also leads to increased errors in the polar stratosphere, hence, tropospheric bias-corrections may degrade the mid-stratosphere. Additionally, in the StratBC experiment there is no significant improvement below 20hPa (midlat) & 50hPa (polar), even though the bias corrections are applied from 100hPa.

The SLP bias is shown in Fig. 1 g–j. Here we see similarities between the CTRL and StratBC, with a large bias in the Aleutian Low, and the FullBC and TropBC, where that Aleutian low bias is reduced. The reduced bias in surface pressure, and structure of the pressure field is a barotropic feature, as shown in the geopotential height at 300hPa in Supplementary Figure 3. Additional details of the bias corrections are included in Supplementary figure 1, where we show the zonal mean zonal wind, and Supplementary figure 2, the zonal mean temperature. Overall, the bias–correction technique is effective at reducing errors in the climatological zonal winds throughout the atmosphere, with similar results for the temperature. The reductions in biases are larger in the extra–tropics than tropics, and the vertical profile of corrections can be effectively controlled.

## 3.2 Teleconnection response to ENSO

We trace the path of ENSO anomalies from the tropical Pacific to the northern hemisphere polar regions and the North Atlantic. Following from Fig. 3 in Jiménez–Esteve and Domeisen, 2019, our Fig. 2 shows the anomalous response of indices chosen to highlight the ENSO teleconnection to the North Atlantic. The El Niño and La Niña forcing does not vary seasonally in our experiments, thus is not shown. ERA5 values are included for reference, although direct comparison with the model runs is difficult due to the idealized experimental setup. The convective response of the tropical atmosphere to SST anomalies is represented by the meridional divergent wind at 100 hPa defined in the region 0°–20°N, 160°–220°E (Fig. 2a). As expected, the positive anomalies for El Niño are greater than the negative La Niño anomalies, however, the ERA5 anomalies are more symmetric ad actually slightly larger for La Niña. We also see there is no significant difference between the experiments. This is not surprising given the small biases in the tropical atmosphere, and reasonably small improvements in the tropics between the control and bias corrected experiments. The anomalous divergence creates a Rossby wave that

leads to a deepening (El Niño) or weakening (La Niña) of the Aleutian low. We measure this using an Aleutian Low Index (ALI), defined as the SLP between 35°–60°N, 180°–240°E, indicated by the green box in Fig. 1 g. The response of the ALI is proportional to the tropical divergence, with the anomalous negative El Niño response being greater than the positive La Niña response. Again, there are no clear differences in the anomalous response between the different climatologies. However, in contrast to the tropical regions, the FullBC and TropBC runs have reduced Aleutian Low biases compared to the CTRL and StratBC runs (Fig. 1 g–j), implying that the response of the Aleutian Low to an ENSO signal is not dependant on model biases. The modelled ALI anomalies are very similar to ERA5.

The next step in the teleconnection is the response of heat flux at 100 hPa, 45°–75°N (HF). The anomalous HF for both El Niño and La Niña shows differences between the climatologies. For an El Niño forcing the CTRL and StratBC runs show an increase in HF with significant values (indicated by black dots) for the DJF and JFM three–month means, whereas the FullBC and TropBC anomalies are about half as strong and have no significant values. The results are almost opposite for the La Niña forcing, except the CTRL and TropBC anomalous HF was around half the value of the StratBC and FullBC runs, and there were no significant HF values for any of the La Niña experiments. The lack of significance could be partly due to the weaker Rossby wave source associated with a La Niña, and the high variability of the HF. All El Niño model runs underestimate HF relative to ERA5, however, the La Niña HF anomalies are actually positive, which is not the canonical response,. It may be due to the low number of events in the observational record.

We measure the response of the stratospheric polar vortex with the zonal mean zonal wind at 60N and 10 hPa (UZ60). UZ60 is well predicted by the HF values. Namely, for an El Niño forcing the CTRL and StratBC experiments show a significant weakening, whereas the response of FullBC and TropBC only show a slight weakening of the vortex (Fig. 2d). Likewise with the La Niña forcing the FullBC and StratBC show a greater strengthening than the CTRL and TropBC. These results are also true for the lower stratosphere as measure with the zonal mean zonal wind at 60N and 100hPa (Fig. 2e). We also show the seasonal mean of the full zonal mean wind response in Supplementary figure 4. As with the ALI response, the response of the polar vortex does not appear to be affected by biases in the strength of the vortex, and is instead fully explained by the heat flux response, which is discussed further in the next section. Comparing the late-winter response in ERA5 to the models, the CTRL and StratBC anomalies are similar to ERA5 at 10hPa, but the FullBC and TropBC anomalies are similar at 100hPa.

The differences in the stratospheric response are not mirrored in the response of the NAO, despite the well-known connection between the vortex and the NAO and the importance of a realistic stratosphere for the ENSO–North Atlantic teleconnection (for example, as shown by Cagnazzo and Manzini, 2009 with a similar model to our study). There is a weaker FullBC response in early winter UZ60 to La Nina, and correspondingly weaker NAO response in early winter. However, for the other runs the strength of the polar vortex anomaly has no clear connection with the response of the NAO. This is evident when comparing the El Niño response of the CTRL and StratBC, to FullBC and TropBC, where the latter two have a weak UZ60 response but a strong NAO response.

To determine the reason for the weak connection between the stratospheric anomalies and the NAO, we investigate scatter plots of uz 60N 10hPa and the NAO index, as shown in Figure 3. For this figure we chose to show the variability within each experiment (i.e. 100 years of DJF means for El Niño, Neutral and La Niña) to better understand the time-mean sensitivity of ENSO teleconnection as well as the sensitivity of the stratosphere-troposphere couplings to different climatologies. The figure shows that there is the expected relationship between UZ60 and the NAO within each experiment – that is, a weaker vortex is associated with a more negative NAO. There is an indication that this relationship is also apparent between the El Niño, and Neutral/La Niña years, with a much smaller signal between the Neutral and La Nina experiments. However, the large variability within each experiment means that the forced difference is relatively small. Although causality is not explained, the figure demonstrates that the stratosphere-troposphere coupling does not play an important role in the ENSO-EU teleconnection in our experiments. The effect is relatively small compared to variability, and hence, the different polar vortex responses between the bias correction experiments do not translate neatly into different magnitudes of the NAO response. One could also hypothesize that a weakened polar vortex response to El Niño in FullBC and TropBC can cause a NAO response of similar magnitude to that in CTRL and StratBC because of an increased sensitivity of NAO to the stratospheric variability. However, the similarity of the UZ60-NAO correlation coefficients between the experiments does not support this hypothesis. Instead, it reveals that the sensitivity of NAO to the stratospheric variability remained unchanged. Overall, for our experiments the stratosphere plays only a minor role in the NAO response.

### 3.3 Difference in polar vortex El Niño response

To investigate the cause of the different HF response between the experiments it is necessary to consider the effect of the bias corrections. To do that we must consider the absolute values and anomalous response together. In Figure 4 we show the DJF ALI, HF and UZ60, for La Niña, Neutral and El Niño conditions. ERA5 is included to demonstrate the biases. Figure 4a shows the reduced bias in the ALI in the FullBC and TropBC experiments compared to the CTRL and StratBC experiments. The figure also shows the deepening and weakening of the ALI for the ENSO forcing is fairly constant between the climatologies, hence, the larger biases in the CTRL and StratBC experiments do not impact the response of the AL. In Figure 4b we again see the reduced bias in the FullBC and TropBC experiments for the HF. However, there is a smaller change between neutral and El Niño conditions for the FullBC and TropBC compared to the CTRL and StratBC. In other words, in the model the HF is less sensitive to the deepening of the AL in the climatologies where the AL is already deeper due to the reduced bias. The same is not true in ERA5, although we caution against using this to dismiss the model results, due to the low number of events (around 8–9 per ENSO phase).

As shown in Fig. 2d, the response of the polar vortex is controlled by the HF response in the different climatologies. Figure 4c reiterates this, and also demonstrates that the biases in the polar vortex do not impact its response to anomalous wave forcing. In neutral conditions the UZ60 biases in the StratBC and FullBC are around 5 m s$^{-1}$ less than the CTRL and TropBC biases. However, for El Niño conditions the FullBC (less bias, stronger vortex) and TropBC (more biased, weaker vortex)

have a weak response, and the StratBC (less bias, stronger vortex) and CTRL (more biased, weaker vortex) have a strong response.

215 We have shown that the stratospheric response to an El Niño forcing is partially dependant on model biases, and seems to be related to the sensitivity of the HF to the AL. In Fig. 5 we use regressions of HF onto SLP to show how the effectiveness of wave forcing by the Aleutian low changes between neutral and El Niño conditions. Similar to Figure 3, we again consider the variability within each bias-correction and ENSO experiment, to understand the time-mean response. Figure 5 a–d shows the regression of monthly HF onto monthly SLP for the extended winter months (November–March) in neutral ENSO

220 conditions. The areas of SLP that are most strongly associated with HF are the Aleutian low region and Siberia, with weaker connections over Greenland and North America. In neutral years these features are very similar between the control and the bias corrected runs, which means the deeper Aleutian low has not affected it's association with wave driving. Figure 5 e–h is the same regression in years with an El Niño forcing. Rather than testing the difference between neutral and El Niño years, this is now a measure of variability during El Niño years. The connection between SLP in the Aleutian low and HF is lower

225 in the CTRL and StratBC El Niño runs, but is now absent in the FullBC run and very weak in the TropBC runs. Therefore, for an equally large AL anomaly, there would be less wave forcing in the FullBC and TropBC. There appears to be a threshold for the depth of the Aleutian Low, below which any additional anomalies do not result in additional wave forcing. During La Niña years the regression values over the AL region are slightly stronger in the FullBC and TropBC, but this did not lead to differences in the response of the HF (i.e. Figure 4 b). The HF was plotted against the AL SLP anomalies to test

230 for a non-linear saturation in the wave forcing by the Aleutian Low (Supplementary Figure 5). For variability within the experiments there is an indication that the relationship between HF and AL breaks down with low AL values, and for the FullBC and TropBC El Niño experiments the relationship actually reverses slightly. Although it does not conclusively explain the differences between the bias correction experiments, it shows that the HF-AL relationship does change in tandem with the absolute value of the AL, and the behaviour is fairly consistent within each set of bias-correction experiments for

235 different ENSO forcings.

**4 Discussion and Conclusions**

By applying a bias–correction technique to the divergence and temperature tendencies of an atmospheric model we have reduced biases in the tropospheric and stratospheric mean states to create various climatologies. With the different climatologies we have performed idealized ENSO forcing experiments to test the role of biases in ENSO teleconnections.

240 There were only small reductions in the bias in the tropics, and there was no difference in the convective response to ENSO between the experiments. Likewise, the anomalous response of the Aleutian low to El Niño and La Niña forcing was similar between the experiments, despite the reduced biases in the Northern hemisphere troposphere. Reduced biases in the Aleutian low SLP did, however, lead to differences in the anomalous upward wave flux associated with a deepened low due to an El Niño forcing. A stronger polar vortex in the experiments with stratospheric bias correction did not affect the anomalous

245 response of the vortex. Hence, we find that reducing certain climatological biases in the surface pressure and wind speed does not significantly affect the response of the Aleutian low to Rossby wave forcing. The response of the polar vortex was also shown to be dependent on the upward planetary wave forcing, and not affected by local biases in the strength of the vortex. However, the model's ability to generate a planetary wave flux may be dependent on biases in surface pressure. Because the NAO response is not sensitive to the stratospheric representation or response, we conclude that in our

250 experiments with SST forcing corresponding to large ENSO events it is dominated by tropospheric teleconnections. This result appears consistent with that by Bell et al. (2009) who also found that for strong ENSO events the tropospheric teleconnections dominate.

Although one motivation behind artificially bias–correcting the model was to investigate how the response to various forcings might improve if the biases were reduced, it should be noted that the ECHAM atmospheric model has already been

255 shown to have a realistic response to an ENSO forcing (Manzini et al. 2006, Cagnazzo and Manzini, 2009). The ENSO teleconnection, and the Siberian snow–polar vortex connection investigated in Tyrrell et al. (2020), are both relevant to seasonal forecasting, but the bias correction technique is unlikely to be used for operational forecasting. Hence, for these experiments the bias corrections are a tool that is used not to improve the response relative to observations, but rather to explore the sensitivity of the response to climatological biases.

260 It was interesting to find that response of the Aleutian low and the stratospheric polar vortex was not affected by the climatological biases that we reduced. These two features are important in the ENSO–to–Europe teleconnection and had large reductions in bias due to the corrections. These features are also both forced by planetary waves; horizontally propagating waves from anomalous convection in the tropical Pacific, or vertically propagating waves from the northern hemisphere troposphere to the stratosphere. Hence, model biases in the depth of the Aleutian low, or the magnitude of the

265 polar vortex winds, do not appear to strongly affect their response to wave forcing.

The control and bias corrected runs differed in the magnitude of wave forcing caused by the deepening Aleutian low due to the El Niño forcing. We theorize that this was due to the relationship between the depth of the Aleutian low and its effectiveness at wave forcing. The two experiments with bias corrections in the troposphere both had a deeper Aleutian low, which was closer observations. Although the magnitude of ALI anomaly was the same, the runs with a deeper Aleutian low

270 had reduced wave forcing for El Niño conditions. Regressions between SLP and HF showed that lower Aleutian low SLP was associated with a decreasing correlation between Aleutian low SLP and HF. Therefore, we speculate that the reduced wave forcing when the troposphere was bias corrected in the FullBC and TropBC, was due to the lower climatological SLP values in the Aleutian low area. It appears that at some threshold of low values of SLP, further anomalies in the Aleutian low do not result in anomalous upward waves. The opposite was not true for the La Niña conditions, since there appears to be no

275 maximum values where the relationship between HF and Aleutian low SLP changes. Additionally, the non–linearity in the El Niño/La Niña atmospheric response (e.g. Frauen et al., 2014) means that the La Niña response is smaller, making it more difficult to distinguish robust differences between the climatologies. By artificially bias correcting an atmospheric model, we have shown that some aspects of ENSO teleconnections are very robust to the specific model biases we corrected, while

more subtle interactions of anomalies with the basic state can impact the overall response. A deeper understanding of the
280 influence of inherent model biases on teleconnections can guide future model development, and also aid in the physical understanding of these important teleconnections.

**Data availability**

The climatological means of all model experiments, for the variables used in this paper are available at:
https://figshare.com/articles/dataset/ECHAM6_Bias_Correction_ENSO/13311623. The full timeseries is available upon
285 request to Nicholas Tyrrell. ERA-Interim and ERA5 data Copernicus Climate Change Service Climate Data Store (CDS,
https://climate.copernicus.eu/climate-reanalysis). The ECHAM6 model is available to the scientific community under a
version of the MPI-M license http://www.mpimet.mpg.de/en/science/models/license/. The HadISST SST and sea ice data are
available from the U.K. Met Office https://www.metoffice.gov.uk/hadobs/hadisst/.

**Author contributions**

290 NLT conducted the model runs, analysis, and wrote the first draft. AYK contributed to the interpretation of the results, and improving the final manuscript.

**Competing interests**

The authors declare that they have no conflict of interest.

**Acknowledgements**

295 The authors would like to acknowledge Sebastian Rast, John Scinocca, Slava Kharin, and Michael Sigmond for invaluable technical and scientific help. N. L. T. and A. Y. K. are funded by the Academy of Finland (Grants 333255, 286298, and 294120).

**References**

Abid, M.A., Kucharski, F., Molteni, F., Kang, I.S., Tompkins, A.M. and Almazroui, M.: Separating the Indian and Pacific
300 Ocean impacts on the Euro-Atlantic response to ENSO and its transition from early to late winter, J. Clim., 34(4), pp.1531-1548, doi: 10.1175/JCLI-D-20-0075.1, 2021

Ayarzagüena, B., Ineson, S., Dunstone, N.J., Baldwin, M.P. and Scaife, A.A.: Intraseasonal effects of el niño–southern oscillation on North Atlantic climate, J. Clim., 31(21), pp.8861-8873, doi: 10.1175/JCLI-D-18-0097.1, 2018.

305

Baldwin, M.P., Stephenson, D.B., Thompson, D.W., Dunkerton, T.J., Charlton, A.J. and O'Neill, A.: Stratospheric memory and skill of extended-range weather forecasts, Sci., 301(5633), pp.636-640, doi:10.1126/science.1087143, 2003.

Bayr, T., Latif, M., Dommenget, D., Wengel, C., Harlaß, J., and Park, W.: Mean-state dependence of ENSO atmospheric

310 feedbacks in climate models, Clim. Dyn., 50, 3171-3194, doi:10.1007/s00382-017-3799-2, 2018.

Bayr, T., Domeisen, D.I.V. and Wengel, C.: The effect of the equatorial Pacific cold SST bias on simulated ENSO teleconnections to the North Pacific and California, Clim. Dyn. 53, 3771–3789, doi:10.1007/s00382-019-04746-9, 2019.

315 Bell, C. J., Gray, L. J., Charlton–Perez, A. J., Joshi, M. M., and Scaife, A. A.: Stratospheric communication of El Niño teleconnections to European winter, J. Clim., 22, 4083– 4096, doi:10.1175/2009JCLI2717.1, 2009.

Brönnimann, S.: Impact of El Niño–southern oscillation on European climate, Reviews of Geophysics, 45, doi:10.1029/2006RG000199, 2007.

320

Butler, A. H., Polvani, L. M., and Deser, C.: Separating the stratospheric and tropospheric pathways of El Niño–Southern Oscillation teleconnections. Environmental Research Letters, 9(2), 9, doi:10.1088/1748-9326/9/2/024014, 2014.

Cagnazzo, C., and Manzini, E.: Impact of the stratosphere on the winter tropospheric teleconnections between ENSO and the

325 North Atlantic and European region, J. Clim., 22, 1223–1238, doi:10.1175/2008JCLI2549.1, 2009.

Chang, Y., Schubert, S. D., Koster, R. D., Molod, A. M., and Wang, H.: Tendency Bias Correction in Coupled and Uncoupled Global Climate Models with a Focus on Impacts over North America, J. Clim., 32 (2), 639–661, doi:10.1175/JCLI-D-18-0598.1, 2019.

330

Domeisen, D. I., Garfinkel, C. I., and Butler, A. H.: The teleconnection of El Niño Southern Oscillation to the stratosphere, Reviews of Geophysics, 57(1), 5-47, doi:10.1029/2018RG000596, 2019.

Dommenget, D., Haase, S., Bayr, T., and Frauen, C.: Analysis of the Slab Ocean El Niño atmospheric feedbacks in observed

335 and simulated ENSO dynamics, Clim. Dyn., 42(11–12), 3187-3205, doi:10.1007/s00382-014-2057-0, 2014.

Frauen, C., Dommenget, D., Tyrrell, N. L., Rezny, M. and Wales, S.: Analysis of the Nonlinearity of El Niño–Southern Oscillation Teleconnections, J. Clim., doi:10.1175/JCLI-D-13-00757.1, 2019.

340   Garfinkel, C. I., and Hartmann, D. L.: Effects of the El Niño–Southern Oscillation and the quasi--biennial oscillation on polar temperatures in the stratosphere, J. Geophys. Res.-Atmos., 112(D19),  doi:10.1029/2007JD008481, 2007.

Garfinkel, C. I., Weinberger, I., White, I. P., Oman, L. D., Aquila, V., and Lim, Y. K.: The salience of nonlinearities in the boreal winter response to ENSO: North Pacific and North America, Clim. Dyn., 52, 4429–4446, doi:10.1007/s00382-018-
345   4386-x, 2019.

Hersbach, H., Bell, B., Berrisford, P., Hirahara, S., Horányi, A., Muñoz–Sabater, J., ... and Simmons, A.: The ERA5 global reanalysis, Q. J. Roy. Met. Soc., 146(730), 1999-2049, doi:10.1002/qj.3803, 2020.

350   Hoskins, B. J., and Karoly, D. J.: The steady linear response of a spherical atmosphere to thermal and orographic forcing. J. Atmos. Sci., 38(6), 1179–1196, doi:10.1175/1520-0469-1981-038, 1981.

Jiménez–Esteve, B., and Domeisen, D. I. V.: The tropospheric pathway of the ENSO–North Atlantic teleconnection, J. Clim., 31(11), 4563–4584, doi:10.1175/JCLI-D-17-0716.1, 2018.
355

Jiménez–Esteve, B., and Domeisen, D. I. V.: Nonlinearity in the North Pacific atmospheric response to a linear ENSO forcing, Geophys. Res. Lett., 46(4), 2271-2281, doi:10.1029/2018GL081226, 2019.

Kharin, V. V., and Scinocca, J. F.: The impact of model fidelity on seasonal predictive skill, Geophys. Res. Lett., 39(18),
360   doi:10.1029/2012GL052815, 2012.

King, M.P., Herceg-Bulić, I., Bladé, I., García-Serrano, J., Keenlyside, N., Kucharski, F., Li, C. and Sobolowski, S.: Importance of late fall ENSO teleconnection in the Euro-Atlantic sector, Bull. Am. Met. Soc., 99(7), pp.1337-1343, doi: 10.1175/BAMS-D-17-0020.1, 2018.
365

Magnusson, L., Alonso-Balmaseda, M., Corti, S., Molteni, F. and Stockdale, T.: Evaluation of forecast strategies for seasonal and decadal forecasts in presence of systematic model errors, Clim. Dyn. 41, 2393–2409, doi:10.1007/s00382-012-1599-2,  2013a.

370     Magnusson, L., Alonso–Balmaseda, M. and Molteni, F.: On the dependence of ENSO simulation on the coupled model mean state, Clim. Dyn., 41, 1509–1525, doi:10.1007/s00382-012-1574-y,  2013b.

Manganello, J. V. and Huang, B.: The influence of systematic errors in the Southeast Pacific on ENSO variability and prediction in a coupled GCM. Clim. Dyn., 32, 1015–1034, doi:10.1007/s00382-008-0407-5, 2009.

375

Manzini, E., Giorgetta, M. A., Esch, M., Kornblueh, L., and Roeckner, E.: The Influence of Sea Surface Temperatures on the Northern Winter Stratosphere: Ensemble Simulations with the MAECHAM5 Model, J. Clim., 19 (16): 3863–3881, doi:10.1175/JCLI3826.1, 2006.

380     Mezzina, B., García-Serrano, J., Bladé, I., Palmeiro, F.M., Batté, L., Ardilouze, C., Benassi, M. and Gualdi, S.: Multi-model assessment of the late-winter extra-tropical response to El Niño and La Niña, Clim. Dyn., 1-22. doi: 10.1007/s00382-020-05415-y, 2020.

Rodríguez–Fonseca, B., Polo, I., García–Serrano, J., Losada, T., Mohino, E., Mechoso, C. R., and Kucharski, F.:. Are
385     Atlantic Niños enhancing Pacific ENSO events in recent decades? Geophy. Res. Lett., 36(20), L20705, doi:10.1029/2009GL040048, 2009.

Simpson, I. R., Hitchcock, P., Shepherd, T. G, and Scinocca, J. F.: Southern annular mode dynamics in observations and models. Part I: The influence of climatological zonal wind biases in a comprehensive GCM, J. Clim., 26, 3953–3967,
390     doi:10.1175/JCLI-D-12-00348.1,  2013a.

Simpson, I. R., Hitchcock, P., Shepherd, T. G, and Scinocca, J. F.: Southern annular mode dynamics in observations and models. Part II: Eddy feedbacks, J. Clim., 26, 5220–5241, doi:10.1175/JCLI-D-12-00495.1, 2013b.

395     Spencer, H., Sutton, R., and Slingo, J. M.: El Niño in a Coupled Climate Model: Sensitivity to Changes in Mean State Induced by Heat Flux and Wind Stress Corrections. J. Clim., 20, 2273–2298,  doi:10.1175/JCLI4111.1, 2007.

Stevens, B., and Co–authors: Atmospheric component of the MPIM Earth System Model: ECHAM6. J. Adv. Mod. Earth Sy., 5 (2), 146–172, doi:10.1002/JAME.20015@10.1002/(ISSN)1942-2466.MPIESM1, 2013.
400

Tyrrell, N. L., Karpechko, A. Y., and Rast, S.: Siberian snow forcing in a dynamically bias–corrected model, J. Clim. 33(24), 10455-10467, doi:10.1175/JCLI-D-19-0966.1, 2020.

**Table 1. Experiment details and run names.**

| Bias corrections | ENSO Neutral | El Niño | La Niña |
|---|---|---|---|
| None | CTRL | CTRL_EN | CTRL_LN |
| 850 hPa to 2.6 hPa | FullBC | FullBC_EN | FullBC_LN |
| 100 hPa to 2.6 hPa | StratBC | StratBC_EN | StratBC_LN |
| 850 hPa to 100 hPa | TropBC | TropBC_EN | TropBC_LN |

405

410
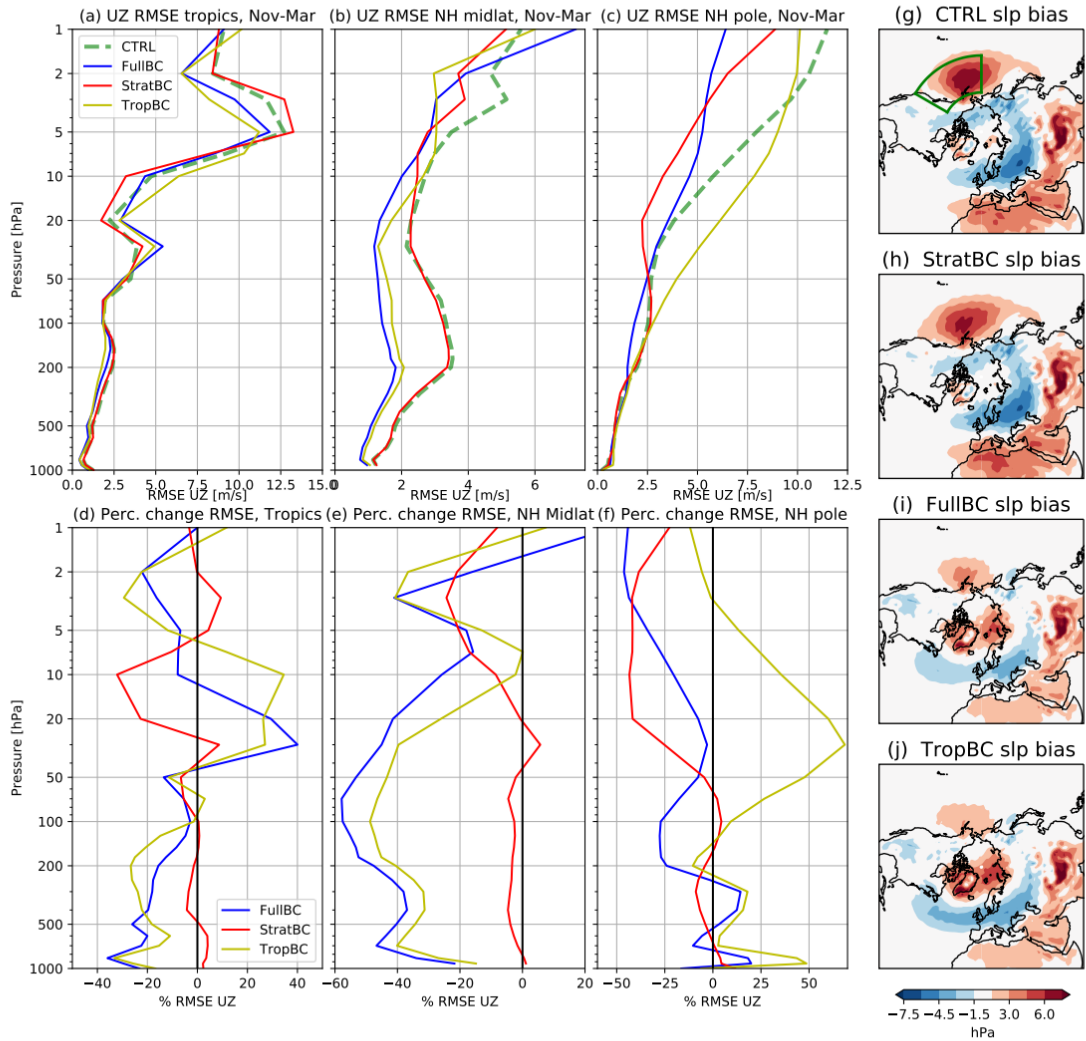
**Figure 1: Panels a–c shows RMSE of UZ in the four experiment, in the tropics (20°S to 20°N), the mid–latitudes (20°N to 50°N) and the pole (50°N to 90°N). RMSE calculated using difference between model and ERA Interim climatology. Panels d–f are the percentage change of UZ RMSE between the control run and the three bias–corrected runs, with negative values showing improvement in the climatology of the bias corrected runs. Panels g–j show the bias in the control and bias corrected experiments, calculated as the experiment minus ERA interim. The green box in (g) shows area of the Aleutian Low Index.**

415
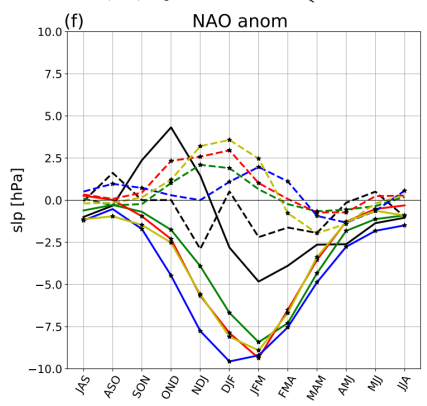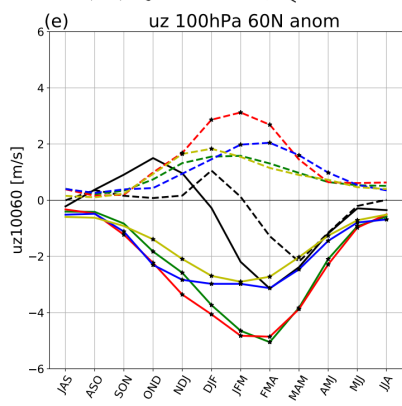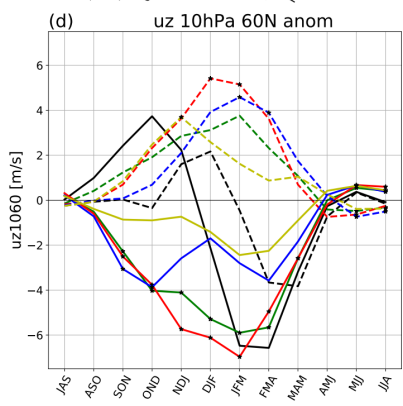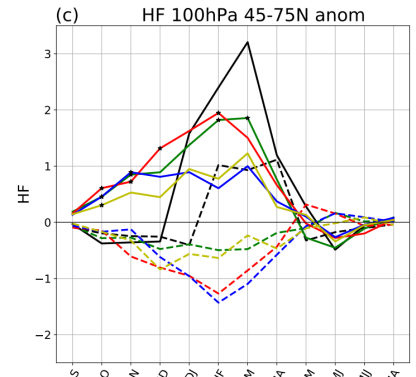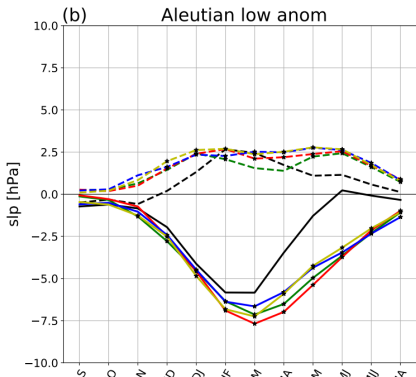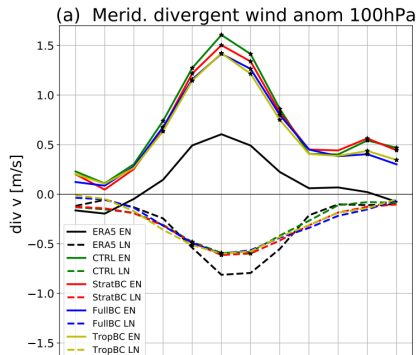
**Figure 2. Progression of anomalies from the ENSO region to the stratospheric polar vortex and NAO, for the model and ERA5.**
Timeseries uses three–month means, and black dots indicate significance at p < 0.05. For model runs solid lines show 100 years of the El Niño run minus 100 years neutral run, dashed lines show 100 years of the La Niña run minus 100 years neutral run. ERA5 anomalies show the difference between a composite of 8 El Niño or La Niña years, and 12 neutral years.

420
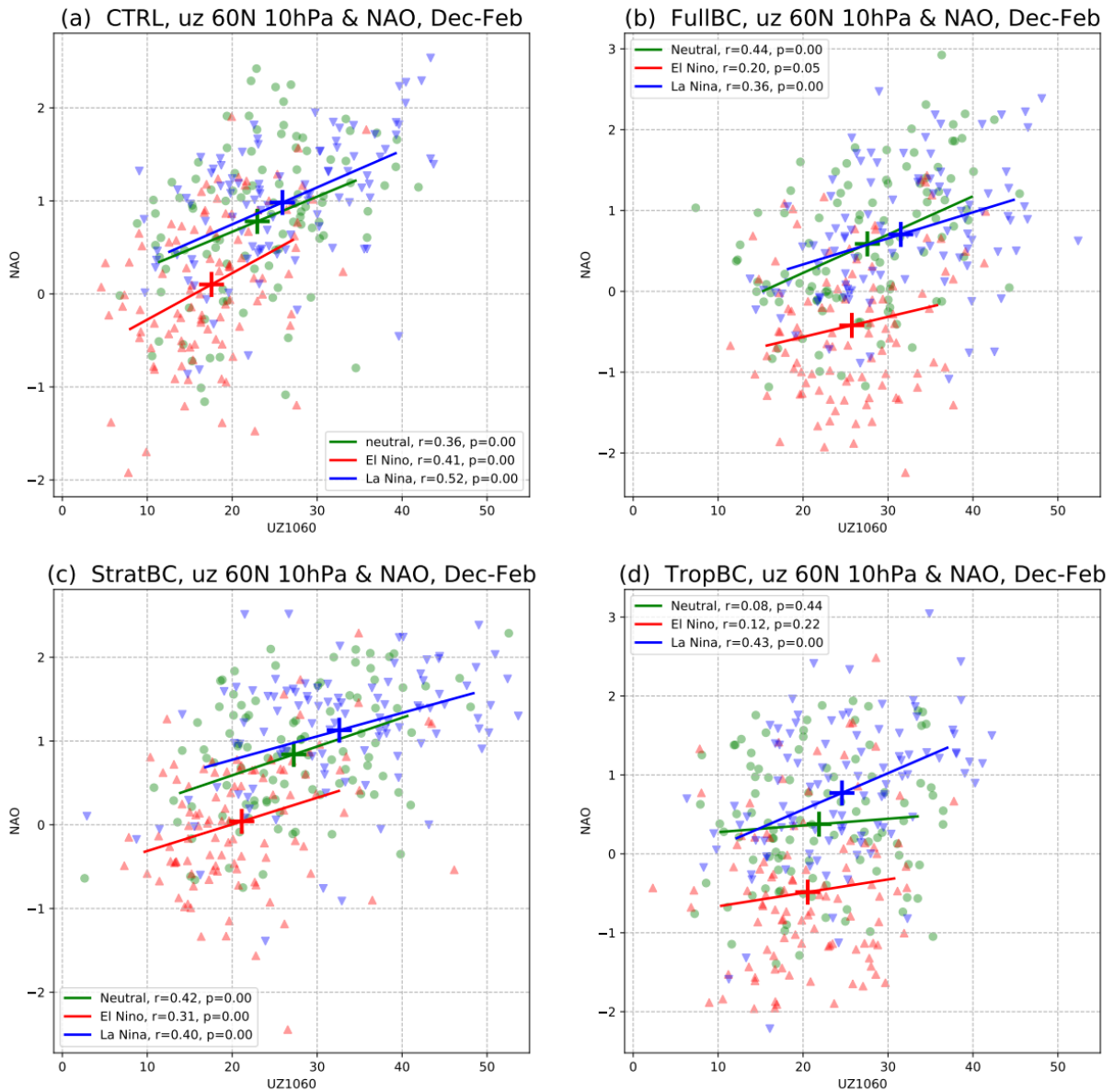
**Figure 3. Scatterplot with regression line of mean DJF values of uz at 60N 10hPa and the NAO index, for (a) CTRL, (b) FullBC, (c) StratBC and (d) TropBC. Neutral years are green, El Niño years are red, and La Niña years are blue. The large crosses indicate the mean value for each El Nino/La Nina/Neutral experiment.**
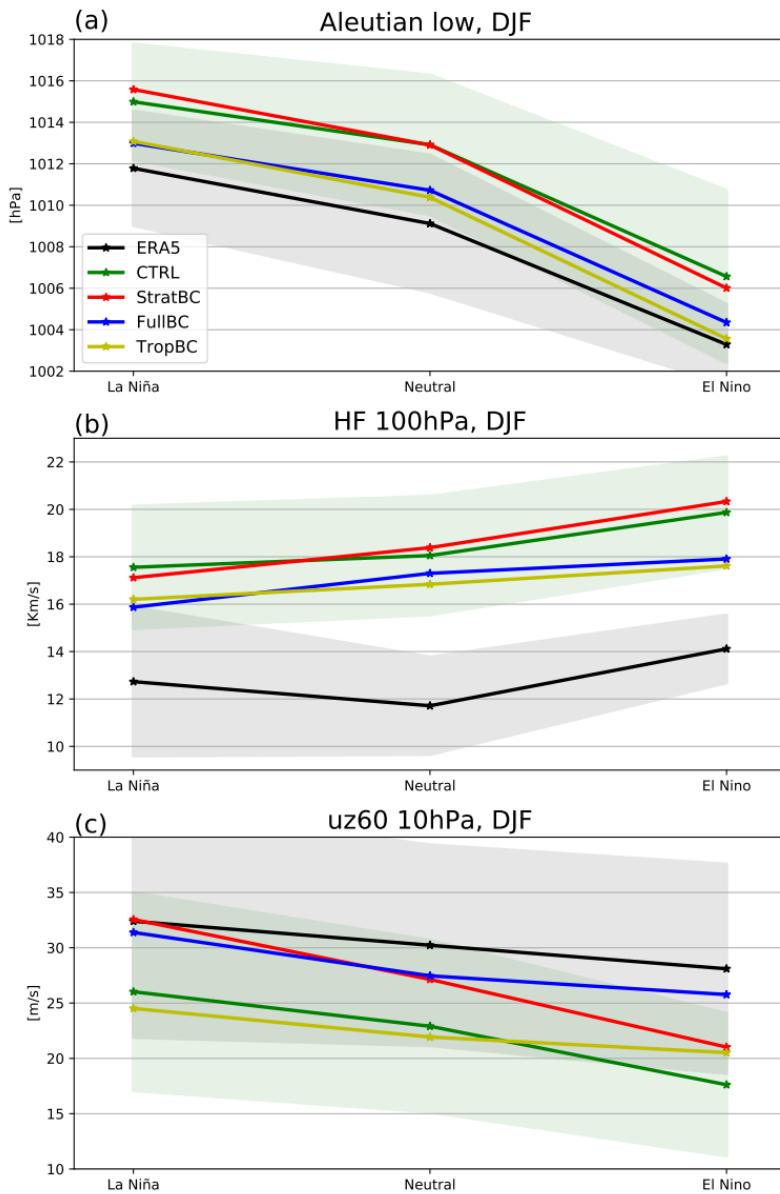
Figure 4. DJF values of (a) Aleutian Low Index, (b) heat flux between 45N–75N at 100 hPa and (c) UZ60 for La Niña, neutral and El Niño years. Shading shows one standard deviation for the CTRL run (green) and ERA5 (grey).
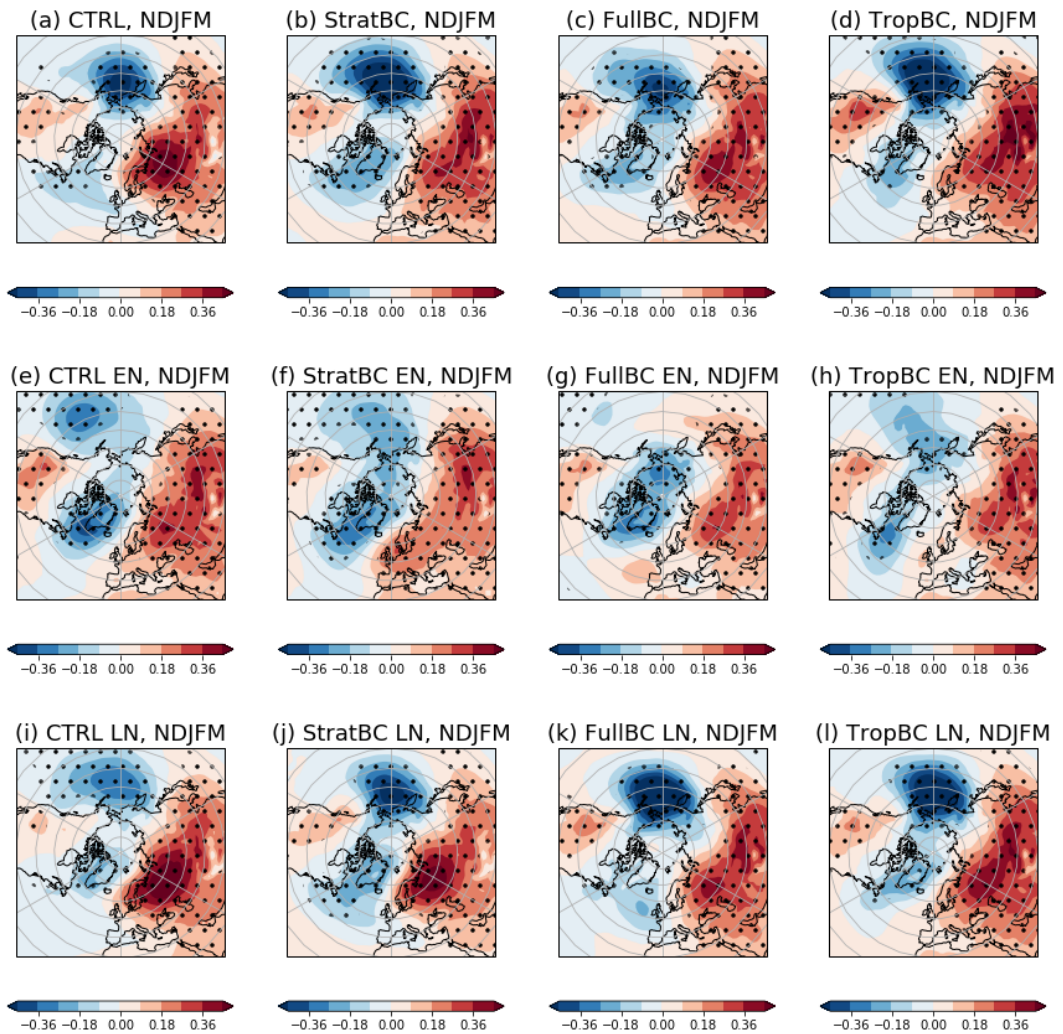
Figure 5. Regression of monthly HF and monthly sea level pressure for extended winter months (Nov–Mar). Top row is neutral years, middle row is El Niño years, bottom row is La Niña years. Stippling indicates significance at p < 0.05.